GeroScience (2024) 46:2503–2519
https://doi.org/10.1007/s11357-023-01014-x

ORIGINAL ARTICLE

# Immune proteins C1q and CD47 may contribute to aberrant microglia-mediated synapse loss in the aging monkey brain that is associated with cognitive impairment

**Sarah A. DeVries · Bryce Conner · Christina Dimovasili · Tara L. Moore · Maria Medalla · Farzad Mortazavi · Douglas L. Rosene**

Received: 25 September 2023 / Accepted: 7 November 2023 / Published online: 22 November 2023


**Abstract** Cognitive impairment in learning, memory, and executive function occurs in normal aging even in the absence of Alzheimer's disease (AD). While neurons do not degenerate in humans or monkeys free of AD, there are structural changes including synapse loss and dendritic atrophy, especially in the dorsolateral prefrontal cortex (dlPFC), and these correlate with cognitive age-related impairment. Developmental studies revealed activity-dependent neuronal properties that lead to synapse remodeling by microglia. Microglia-mediated phagocytosis that may eliminate synapses is regulated by immune "eat me" and "don't eat me" signaling proteins in an activity-dependent manner, so that less active synapses are eliminated. Whether this process contributes to age-related synapse loss remains unknown. The present study used a rhesus monkey model of normal aging to investigate the balance between the "eat me" signal, complement component C1q, and the "don't eat me" signal, transmembrane glycoprotein CD47, relative to age-related synapse loss in dlPFC Area 46. Results showed an age-related elevation of C1q and reduction of CD47 at PSD95+ synapses that is associated with cognitive impairment. Additionally, reduced neuronal CD47 RNA expression was found, indicating that aged neurons were less able to produce the protective signal CD47. Interestingly, microglia do not show the hypertrophic morphology indicative of phagocytic activity. These findings suggest that in the aging brain, changes in the balance of immunologic proteins give microglia instructions favoring synapse elimination of less active synapses, but this may occur by a process other than classic phagocytosis such as trogocytosis.

**Keywords** Synapse · Microglia · C1q · CD47 · Aging · Cognitive decline

S. A. DeVries (✉) · B. Conner · C. Dimovasili · T. L. Moore · M. Medalla · F. Mortazavi · D. L. Rosene
Laboratory for Cognitive Neurobiology, Department of Anatomy & Neurobiology, Boston University Chobanian & Avedisian School of Medicine, Boston University Medical Campus, Boston, MA, USA
e-mail: sdevries@bu.edu

T. L. Moore · M. Medalla · D. L. Rosene
Center for Systems Neuroscience, Boston University, Boston, MA, USA

## Introduction

Starting in early adulthood, humans may begin to exhibit declines in processing speed, learning, memory, and executive function that all continue to deteriorate with age [1]. About 30% of individuals will exhibit severe cognitive impairment with age despite a lack of pathological insults that are present in neurodegenerative diseases, such as Alzheimer's disease (AD) [2]. Given the increasing lifespan and growing aged population, it is important to understand causes of age-related cognitive decline so they can be targeted by new therapeutics to slow decline. Studies

investigating the neurobiological underpinnings of normal aging show stable neuron numbers in aging humans free of AD [3], so simple neuron loss cannot account for this age-related cognitive impairment [4–6]. Instead, structural changes occur in existing neurons and their axons, leading to disrupted connectivity. One area particularly vulnerable to aging in humans is Area 46, or the dorsolateral prefrontal cortex (dlPFC), as it is among the first brain regions to show signs of volume loss and ultrastructural disturbances [1, 7]. Correspondingly, the cognitive domains for which the dlPFC is critical, such as working memory and executive function [8–10], are among the first cognitive domains to show impairment with age [11–13].

Monkeys are a valuable model for studying normal human aging and have provided considerable insight into underlying changes associated with cognitive impairment. Monkeys exhibit age-related cognitive impairment in learning, executive function, and memory [14–16] similar to humans, but remain free from AD, which often confounds studies of normal human aging [16, 17]. Additionally, monkey brain circuitry closely resembles that of humans, and their brains can be optimally preserved for histochemical analyses [16, 17]. As in humans, normal aging rhesus monkeys exhibit stable neuron numbers across the life span [18, 19], but structural disturbances such as synapse loss and myelin pathology have been reported [20–23]. Specifically, ultrastructural studies in our lab's monkey model of human aging reveal dendritic atrophy and synapse loss in layers 1, 2, 3, and 5 in the dlPFC gray matter [18, 20, 24] as well as electrophysiological changes to pyramidal neurons in layer 3 including hyperexcitability and increased input resistance which are associated with age-related cognitive decline and spatial working memory deficits [21, 22, 25].

Studies in aging monkeys have revealed activity-dependent neuronal properties, such as spine plasticity or axonal damage, that lead to synapse remodeling [7, 26], but the mechanism behind age-related synapse loss remains largely unknown. Given the importance of glia in synapse maintenance, one key question is whether synapses are aberrantly eliminated in aging by microglia, the resident immune cell of the central nervous system. The aging brain exhibits chronic inflammation, and microglia exhibit phagocytic morphologies and inflammatory phenotypes that prime them for phagocytosis [27–29]. Interestingly, innate immune signals regulate microglia phagocytosis to maintain homeostasis, including regulation of synaptic connections. Initiating signals, including classical complement components, direct microglia phagocytosis in an activity-dependent manner during developmental synaptic remodeling, allowing more active synapses to be strengthened [30–32].

Of these innate immune signals, the classical complement signal C1q initiates a cascade of downstream signaling and recruits proteins, such as C3, to bind on the target needing removal and directly interact with complement receptor 3 (CR3) on microglial cells [33, 34]. However, microglia are also directed by inhibitory signals, deemed "don't eat me" signals, that protect against unnecessary phagocytosis. "Don't eat me" protein CD47 has been shown to preferentially localize to more active synapses in the developing retina to inhibit excess phagocytosis [35]. Thus, the vulnerability to phagocytosis appears to depend on the balance of tagging from "eat me" signals as well as "don't eat me" signals as shown by in vitro experiments [36]. Therefore, during aging, an increase in cytokines and inflammatory markers along with diminished protective signals may encourage synapse elimination in the presence of inflammatory microglia primed for phagocytosis, causing aberrant removal. During normal aging, it has been shown in both mice and monkeys that C1q is increased at neuronal synapses [37, 38]. However, inhibitory signals that reduce phagocytosis have yet to be investigated during aging to our knowledge.

To determine if the balance between C1q and CD47 in the dlPFC changes during normal aging to favor phagocytosis and how these changes correlate with age-related synapse loss and cognitive impairment, we examined fixed frozen brain sections from 32 cognitively characterized rhesus monkeys. We hypothesized that synapses would be lost with age, and that aged neurons would be less capable of expressing protective CD47, resulting in existing synapses having less CD47 and more C1q localized to their membranes, thus leaving them vulnerable to microglial phagocytosis. To evaluate this, we used multi-label immunohistochemistry (IHC) to assess the presence of C1q and CD47 at synapses in the dlPFC and in situ hybridization to assess the RNA expression of CD47 in neurons. Finally, we used IHC to evaluate the status of microglia in the brain.

## Methods

### Subjects

Archived cryopreserved brain tissue was used from 32 male and female rhesus monkeys ranging from 7 to 30 years old (Fig. 1a) that were behaviorally tested as described below. Prior to euthanasia, monkeys were maintained in the Animal Science Center on Boston University Medical Campus (BUMC), which is fully accredited by AAALAC and managed by a licensed veterinarian staff. All procedures conformed to the NIH Guide for the Care and Use of Laboratory Animals and were approved by the Boston University Institutional Animal Care and Use Committee (IACUC). In the study, water was available ad libitum and chow, fruit, vegetables, and forage feed were given after behavioral testing was complete for the day.

### Cognitive testing

All monkeys were cognitively assessed for learning, recognition memory, working memory capacity, and executive function. The battery of cognitive tests included delayed non-match to sample (DNMS) acquisition and 120-s delay phases, the spatial modality of delayed recognition span task (DRST), and the Category Set Shifting Task (CSST). The details of these can be found in [12, 14, 15, 39–42]. Previous research revealed a combination of DNMS-acquisition, DNMS-120-s delay, and DRST-spatial provided

**a**

| ID | AGE | CII | Sex |
|---|---|---|---|
| AM222 # | 7.4 | 0.871 | M |
| AM280 # | 8.1 | 1.244 | M |
| AM358 # | 8.4 | 0.247 | F |
| AM299 # | 8.6 | 0.850 | F |
| AM296 # | 8.7 | 0.774 | M |
| AM368 | 8.9 | 0.933 | M |
| AM289 # | 9.0 | 0.325 | M |
| AM255 # | 9.5 | 0.123 | F |
| AM294 | 9.6 | 2.215 | F |
| AM295 | 10.8 | 1.523 | M |
| AM291 | 13.7 | 1.172 | F |
| AM353 | 14.5 | 1.053 | M |
| AM303 | 15.2 | 1.168 | M |
| AM288 | 16.0 | 3.148 | M |
| AM378 | 16.8 | 4.115 | M |
| AM297 | 18.0 | 1.152 | F |
| AM274 | 18.3 | 2.284 | M |
| AM300 | 19.0 | 0.804 | F |
| AM293 | 19.6 | 2.097 | F |
| AM372 | 20.8 | 2.853 | M |
| AM287 # | 21.2 | 2.407 | F |
| AM286 | 22.4 | 1.429 | F |
| AM242 | 23.5 | 2.099 | M |
| AM356 # | 24.8 | 2.471 | M |
| AM283 | 26.4 | 2.847 | M |
| AM371 # | 26.6 | 1.966 | F |
| AM306 # | 26.7 | 5.323 | F |
| AM298 # | 26.7 | 1.279 | M |
| AM369 # | 27.0 | 3.193 | F |
| AM370 # | 27.5 | 1.074 | F |
| AM355 # | 28.3 | 3.905 | M |
| AM373 # | 30.2 | 4.971 | M |

# denotes animals used in RNAscope study

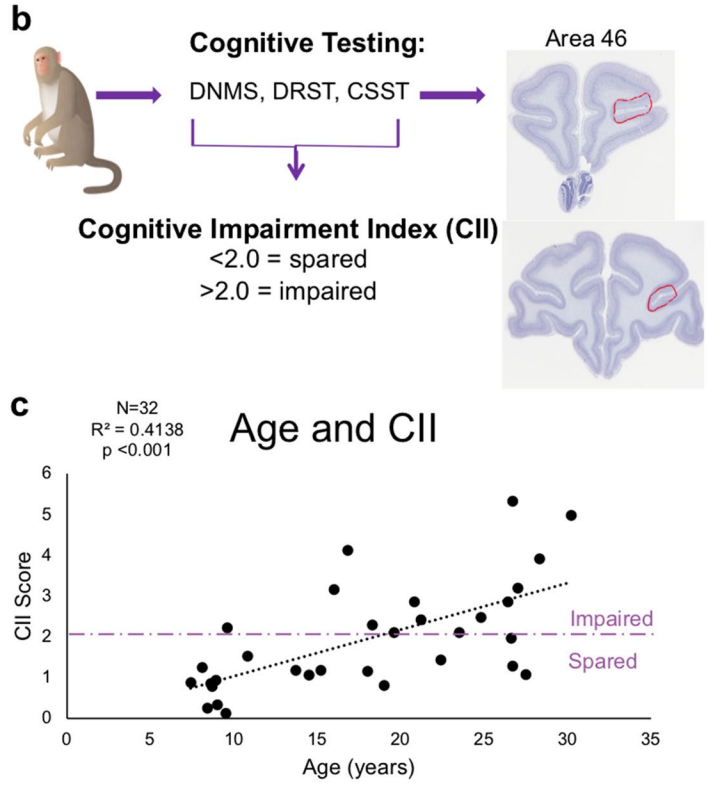


**Fig. 1** Summary of subjects and experimental parameters. **a** Table listing the 32 monkeys' IDs, age, CII, and sex used for these experiments. Animals denoted with # were the 16 subjects used for the *C1qA* and *CD47* RNAscope experiment. **b** Schematic summarizing behavioral tasks, cognitive characterization, and the dlPFC region of interest examined. **c** Linear regression of significant cognitive impairment, measured by CII score, with age for this cohort of subjects. Purple dashed line indicates the cognitive impairment cut off, where subjects above the line are severely impaired and those below are cognitively spared

a sensitive measure of cognitive deficits during aging [12], and therefore, we computed an average of these three tasks by converting them into *z*-scores relative to the mean of 29 young adult monkeys. This composite is termed the cognitive impairment index (CII). Monkeys with impairment scores < 2.0 are considered cognitively spared successful agers while those with scores > 2.0 are considered impaired unsuccessful agers [12, 14]. The distribution of CII scores for this cohort of 32 monkeys is shown in Fig. 1c and shows significant cognitive impairment with age.

### Delayed non-match to sample

DNMS assesses learning and recognition memory. Subjects first learn to distinguish a novel object from a recently presented familiar object after a 10-s delay. Once the rule is learned to a criterion of 90% correct responses over 100 trials, subjects transition to DNMS-120-s delay, which introduces a 120-s delay between exposure to the familiar object and the recognition trial with a novel object to assess the recognition of the novel object.

### Delayed recognition span task

The spatial modality of DRST assesses working memory capacity by requiring subjects to remember an increasing number of locations of serially placed objects in order to identify the novel location. For each trial of this task, one identical object is added to the previously presented set in a novel location until the novel location is incorrectly identified. The spatial locations are pseudorandomized and the same for all subjects, and the average score is calculated based on the number of trials correct prior to an error.

### Category Set Shifting Task

This adaptation of the human Wisconsin Card Sorting task measures abstraction, set shifting, and perseveration by requiring animals to learn a rule for a given stimulus category, and once this rule is learned, they must shift to a new stimulus category in order to receive a reward [39, 40]. While several outcome measures for CSST have been used, we analyzed total broken sets and perseverative errors out of total errors based on previous research in our lab showing these measures are sensitive to age-related changes [39, 40, 43].

### Brain harvesting

After completing the cognitive test battery, subjects are perfused to harvest brain tissue, as described [44, 45]. First, the animal is deeply anesthetized, the chest opened, and the ascending aorta cannulated through the heart. Then, 2–6 L of Krebs buffer (pH 7.4, 4 °C) are transcardially perfused to flush vasculature and rapidly cool the brain. During this perfusion fresh, unfixed biopsy samples are taken from the left hemisphere. Following this, the right hemisphere is perfused with 4% paraformaldehyde (PF) at 37 °C for 10 min to ensure full fixation. The brain is blocked in situ in the coronal plane, postfixed overnight in 4% PF at 4 °C, and cryoprotected in 10% and then 20% glycerol with 2% DMSO and 0.1 M buffer after which it is flash frozen by immersion in − 75 °C isopentane. It is stored at − 80 °C until cut on a sliding microtome into 10 interrupted series of 30-µm sections. These sections are collected into phosphate buffer with 15% glycerol, except one series is collected in the 15% glycerol with an additional 1% PF to ensure optimal RNA preservation. All series are stored at − 80 °C until removed together for batch processing. This cryopreservation procedure preserves integrity for histochemical processing, including IHC and in situ hybridization [44, 45].

### Immunohistochemistry

To assess synapse loss and colocalization of C1q and CD47 at existing synapses, a multi-label immunohistochemistry (IHC) using antibodies to postsynaptic density 95 (PSD95), neuronal marker NeuN, C1q, and CD47 was performed using sections of the dlPFC that included Area 46 (Fig. 1b). Another experiment assessing the morphology of microglia was performed with an antibody to Iba1 (a pan microglial marker) combined with antibody to P2RY12 in the same fluorescent channel to enhance staining of distal, finer microglia processes as previously described [46, 47]. Additionally, to identify a subpopulation of C1q-positive microglia cells, C1q was added since microglia are the largest source of C1q production [48].

For each subject, 4–6 sections containing Area 46 in the bank of the sulcus principalis spaced 2400 µm apart were used (Fig. 1b). All tissue was removed from − 80 °C, thawed at room temperature, and batched processed. Sections were washed with 0.05 M Tris-buffered saline (TBS) at pH = 7.60 to remove glycerol followed by antigen retrieval to break any cross links that may have formed during fixation with 10 mM sodium citrate buffer (pH = 6.0) in a microwave tissue processor (PELCO Biowave, Ted Pella, Inc. Redding, CA) for 2 × 5 min at 550W and 50 °C and allowed to return to room temperature for 1 h. Sections were blocked in 10% normal donkey serum (NDS; Sigma-Aldrich) and 0.1% Triton-X (Tx) for 1 h at room temperature followed by incubation in primary antibody solution (2% NDS and 0.05% Tx in 0.05 M TBS) along with primary antibodies goat PSD95 (1:1000; Abcam, cat# ab12093), chicken NeuN (1:1000; Abcam, cat# ab134014), mouse C1q (1:400; Abcam, cat# ab71940), rabbit CD47 (1:500; Abcam, cat# ab218810), rabbit Iba1 (1:500; Wako, cat# 019–19741), and rabbit P2RY12 (1:250; Abcam, cat# ab183066). To enhance antibody penetration, tissue was initially microwaved at 150W, 30 °C, 2 × 5 min in the primary antibody solution and then incubated at 4 °C for 48 h. Sections were treated with AlexaFluor 488 donkey anti-goat IgG (1:1000; Thermo Fisher Scientific, MA), CF543 donkey anti-chicken IgY (1:1000; Biotium), AlexaFluor 568 donkey anti-mouse IgG2b (1:500), AlexaFluor 647 donkey anti-rabbit IgG (1:500), AlexaFluor 488 goat anti-rabbit (1:1000), and AlexaFluor 568 goat anti-mouse IgG2b (1:500). Sections were mounted, coverslipped with antifading polyvinyl alcohol DABCO (Sigma-Aldrich, #10,981) mounting media, and stored at 4 °C until removed for imaging. For the microglia morphology IHC, sections were processed as above, but with normal goat serum (NGS).

Images were acquired with a 40 × oil immersion objective lens on a Leica TCS SP8 confocal microscope. For both experiments, a tilescan montage was taken with a *z* stack of 5 images for the quadruple label and 17 images for the microglia experiment in order to capture the entirety of microglia morphology and captured both the dorsal and ventral banks of the dlPFC. One animal was excluded from analyses from the quadruple label due to setting errors on the confocal that led to photobleaching. Images were systematically randomized and those selected were thresholded to the same numbers and analyzed for protein % area with particle analysis and for particle colocalization with the colocalization threshold plugin on ImageJ. Microglia morphology and C1q + / − cells were counted on StereoInvestigator software using stereologic rules. Briefly, microglia soma within the counting box and touching inclusion borders were counted while those outside the counting box or touching the exclusion borders were not counted. Iba1 + cells were classified according to morphology as ramified C1q +, ramified C1q −, hypertrophic C1q +, and hypertrophic C1q −. The density of each cell classification was calculated.

## RNAscope

A subset of 16 subjects was selected (8 male and 8 females with a CII range 0.123–5.323) for RNAscope analysis of *C1qA* and *CD47* expression (Fig. 1a). Animals were grouped as young (7–9 years old; $n = 7$) or old (21–30 years old; $n = 9$) and cognitively spared (CII < 2.0) or cognitively impaired (CII > 2.0). RNAscope hybridizations were carried out using the RNAscope Multiplex Fluorescent Manual Assay kit according to the manufacturer's instructions (Advanced Cell Diagnostics; ACD). Briefly, tissue sections cryopreserved in 0.1 M buffer with 15% glycerol and 1% PF were thawed from − 80 °C, and the dlPFC was dissected from one representative section per animal. Sections were treated with $H_2O_2$ for 10 min at room temperature, before they were mounted on SuperFrost Plus microscope slides (Fisher Scientific, MA). Target retrieval was performed by a 5-min incubation in Target Retrieval reagent (ACD, CA) at 95 °C, followed by a 30-min incubation in Protease Plus (ACD, CA) at 40 °C in the HybEZ II oven. Tissue was incubated with the primary probe *C1qA* (1,200,891-C1, ACD, CA) and probe *CD47* (1,200,901-C2, ACD, CA) for 2 h at 40 °C and stored overnight in 5 × SCC hybridization buffer. The following day, tissue was treated with three probe amplification steps (AMP1-AMP3) and fluorophore conjugation (ACD, CA). *C1qA* probe was labeled with fluorophore Opal-520 nm (Akoya Biosciences, MA) diluted 1:1000 in TSA buffer (ACD, CA), while the *CD47* probe was labeled with fluorophore Opal-690 nm (1:300; Akoya Biosciences, MA). Positive and negative controls, where tissue

was incubated with appropriate probe mixes from ACD (custom cocktail of #521,081, 461,341, and 457,711 housekeeping probes, and negative control mix #320,871, respectively), were included for quality control.

Immediately after RNAscope processing, tissue was blocked in SuperBlock (Thermo Fisher Scientific, MA) for 1 h at 40 °C, and then processed for immunofluorescent labeling by incubating the sections in rabbit Iba1 (1:250; Wako, cat# 019–19741) and chicken MAP2 (1:500; Abcam, cat# ab5392) antibodies in TBS with 0.5% SuperBlock and 0.3% Tx for 1 h at 40 °C. All slides were treated with AlexaFluor 568 donkey anti-rabbit (1:500, Thermo Fisher Scientific, MA) and biotinylated goat anti-chicken (1:500, Vector Laboratories, Burlingame, CA) secondaries for 1 h at 40 °C, followed by 1 h of incubation in Streptavidin AlexaFluor 405 conjugate (1:250; Thermo Fisher Scientific, MA) at 40 °C and finally coverslipped with Prolong Gold mounting medium (Thermo Fisher Scientific, MA).

Images were acquired using a Zeiss LSM 710 NLO confocal microscope. A tilescan of 7 *z*-stacks were taken with a 40 × oil immersion objective lens from both the dorsal and ventral bank of the dlPFC for each sample. Images were analyzed manually by first identifying 100–120 Iba1 + and MAP2 + cells and then counting the RNA puncta located within the soma of each cell.

### Statistics

Data were analyzed using SPSS (SPSS Statistics Version 27.0.1) with an $\alpha \leq 0.05$ for all analyses. Linear regressions were run to assess associations of age and cognitive impairment (CII score, CSST total broken sets, and CSST perseverative errors/total shift errors) as continuous variables with dependent variables of PSD95, C1q, and CD47% area and % colocalization as well as for Iba1 morphology and C1q + / − quantification. Cortical layers 1–6 were analyzed as individual regions of interest. RNAscope data were analyzed with age and cognitive status as discrete variables. Data are shown as the mean ± SEM and differences were analyzed using a two-tailed independent samples *t*-test.

## Results

### Synapse loss occurs during aging and correlates with cognitive decline

Spine and synapse loss are well documented in aging [7, 20, 49]. Here, we labeled the postsynaptic marker PSD95, which labels the scaffolding protein found in all cortical excitatory glutamatergic synapses [50], together with immune markers C1q and CD47 (Fig. 2a–d). Analyses showed a significant excitatory synapse loss, marked by a decrease in PSD95, across the dlPFC cortical gray matter with age [$F(1,30) = 11.380$, $R^2 = 0.275$, $p < 0.05$] that also correlated with increasing cognitive impairment (higher CII score) [$F(1,30) = 8.007$, $R^2 = 0.211$, $p < 0.05$]. To determine if this synapse loss is driven by loss in a specific cortical layer, cortical layers were separated based on neuronal NeuN laminar staining. As shown in Table 1, there was significantly decreased PSD95% area across cortical layers 1–6 with age (Fig. 2e). This synapse loss significantly correlated with cognitive impairment, measured by the CII score, in layers 2–5 but not layer 1 or layer 6, as shown in Table 1, (Fig. 2f). There was no correlation with CSST total broken sets and % area PSD95 (data not shown). However, increased perseverative errors out of total errors correlated with % area of PSD95 loss in layer 3 ($p = 0.031$). These data confirm previous findings of robust synapse loss across cortical layers with age that correlates with cognitive decline in layers 2–5 [7, 20, 26, 49].

### Increased C1q and decreased CD47 are associated with age and age-related cognitive decline

To determine if changes in complement cascade initiator C1q occur with age, we analyzed C1q with an antibody that targets the collagen-like region of the C1q molecule that has been previously shown to be highly specific in several different tissues, including monkey brain tissue, for IHC and immunoblots [37, 51, 52]. Additionally, we used an antibody against CD47, previously used in human tissue [53], to demonstrate changes with age and cognitive impairment. Results showed that C1q increased with age [$F(1,29) = 39.570$, $R^2 = 0.577$, $p < 0.001$] and with cognitive impairment [$F(1,29) = 12.706$, $R^2 = 0.305$, $p < 0.05$]. In contrast, CD47 decreased with age [$F(1,29) = 27.891$,

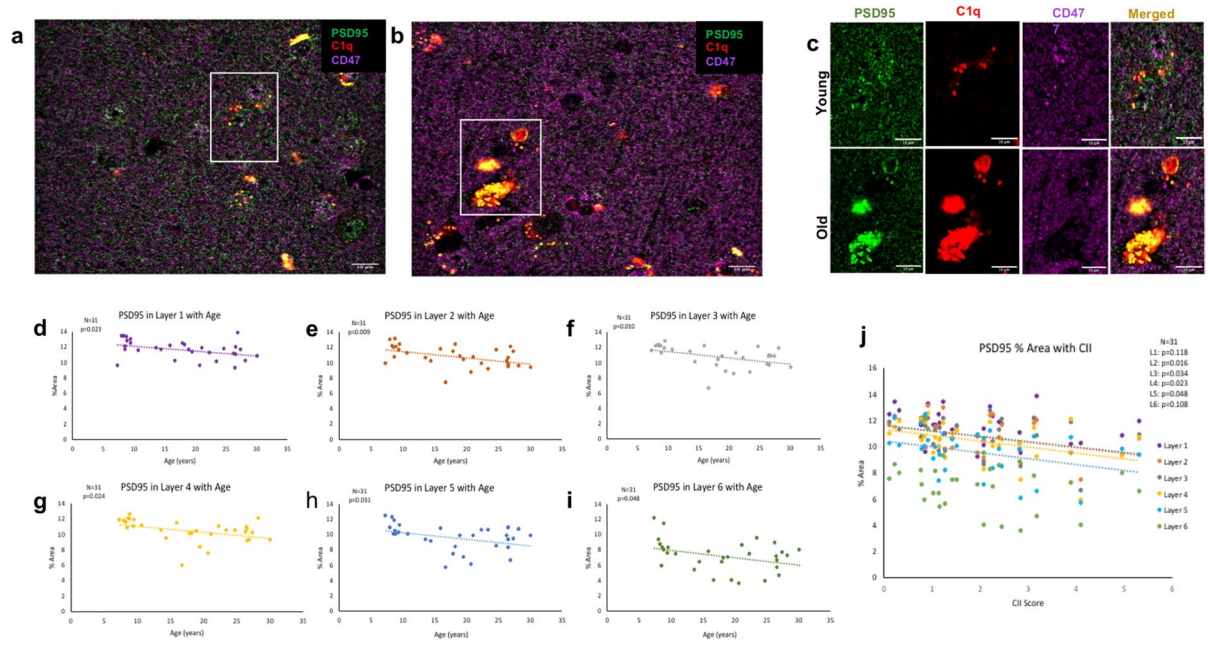


**Fig. 2** PSD95+ synapse % area with age and cognitive impairment. Example post synaptic marker PSD95, C1q, and CD47 immunohistochemical images in (**a**, **c**) young vs (**b**, **c**) old subjects. (**d–i**) Linear regression showing significant PSD95+ synapse loss with age across cortical layers 1–6. (**j**) Synapse loss correlates with cognitive impairment, measured by the cognitive impairment index (CII) in cortical layers 2–5. Scale bar represents 10 µm

**Table 1** Summary of statistics for % area of PSD95 associated with age and CII in cortical layers 1-6

| | Layer 1 | Layer 2 | Layer 3 | Layer 4 | Layer 5 | Layer 6 |
|---|---|---|---|---|---|---|
| PSD95 and age | $F(1,29)=5.730$ | $F(1,29)=7.825$ | $F(1,29)=5.164$ | $F(1,29)=5.696$ | $F(1,29)=5.164$ | $F(1,29)=4.283$ |
| | $R^2=0.165$ | $R^2=0.212$ | $R^2=0.151$ | $R^2=0.164$ | $R^2=0.151$ | $R^2=0.129$ |
| | $p<0.05$ | $p<0.05]$ | $p<0.05$ | $p<0.05$ | $p<0.05$ | $p<0.05$ |
| PSD95 and CII | $F(1,29)=2.593$ | $F(1,29)=6.493$ | $F(1,29)=4.944$ | $F(1,29)=5.743$ | $F(1,29)=4.278$ | $F(1,29)=2.751$ |
| | $R^2=0.082$ | $R^2=0.183$ | $R^2=0.146$ | $R^2=0.165$ | $R^2=0.129$ | $R^2=0.087$ |
| | $p=0.118$ | $p<0.05$ | $p<0.05$ | $p<0.05$ | $p<0.05$ | $p=0.108$ |

$R^2=0.490$, $p<0.001$] and with increasing CII score [$F(1,29)=8.134$, $R^2=0.219$, $p<0.05$]. When we analyzed these proteins according to cortical layer, we found significant elevation in C1q across layers 1–6 with age (Fig. 3a) as well as significant loss of CD47 across layers 1–6 with age, as displayed in Table 2, (Fig. 3b).

As shown in Table 2, C1q increase correlated with cognitive impairment in cortical layers 1–6 (Fig. 3c). Interestingly, CD47 decrease correlated with cognitive impairment in layers 3–6 but not in cortical layers 1 or 2, as shown in Table 2, (Fig. 3d). There was no correlation with CSST total broken sets or % of perseverative errors out of total errors and C1q % area (data not shown). CSST total broken sets correlated with CD47 loss in layer 3 ($p=0.049$) Overall, results show that the increase in C1q and concomitant decrease in CD47 may shift the balance towards greater phagocytosis across all cortical layers in the dlPFC in aging, which correlates with increasing cognitive impairment.

## Age-related changes in C1q-PSD95 and CD47-PSD95 colocalization favor synapse elimination conditions

To determine if the increase in C1q labeling is due to C1q tagging (and phagocytic priming) of synapses,

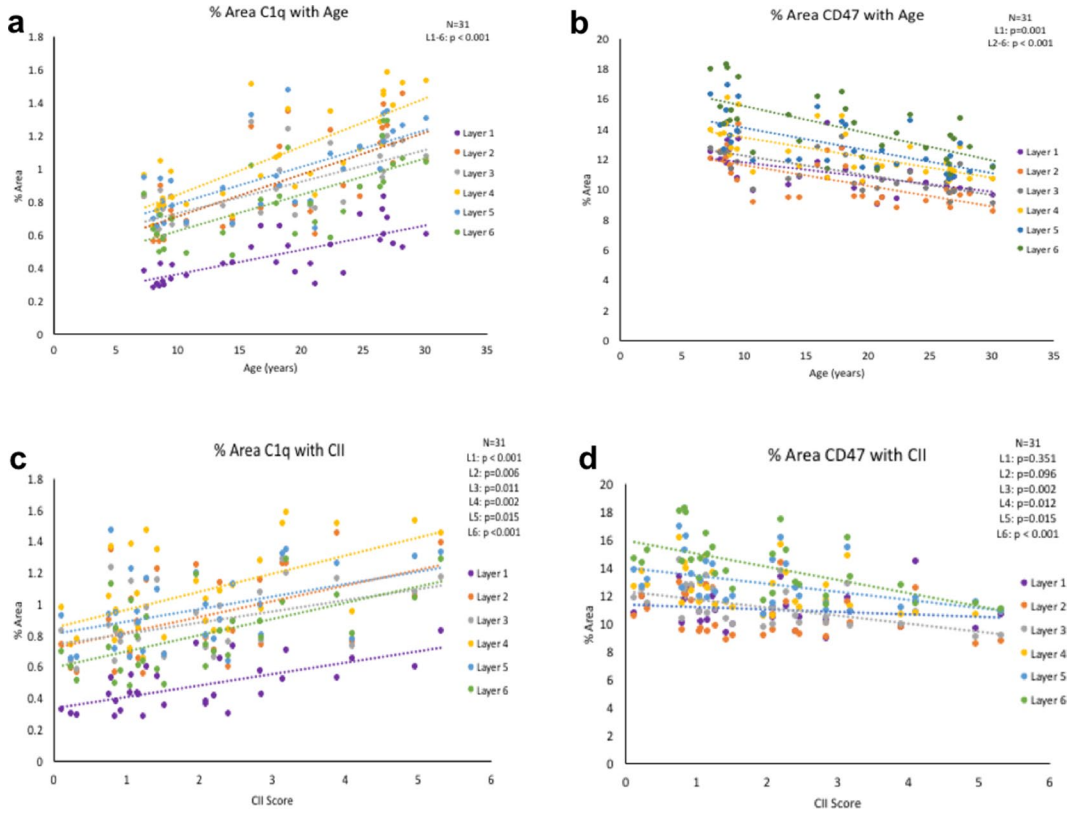


**Fig. 3** C1q and CD47 with age and cognitive impairment. (**a**) % area of C1q increases in cortical layers 1–6 with age. (**b**) CD47 % area decreases in all six cortical layers with age. (**c**) C1q increases with cognitive impairment in layers 1–6. (**d**) CD47 decreases are associated with cognitive impairment in layers 2–5

**Table 2** Summary of statistics for % area of C1q and of CD47 associated with age and CII in cortical layers 1-6

| | Layer 1 | Layer 2 | Layer 3 | Layer 4 | Layer 5 | Layer 6 |
|---|---|---|---|---|---|---|
| C1q and age | [F(1,29) = 32.304<br>$R^2 = 0.527$<br>$p < 0.001$ | F(1,29) = 27.567<br>$R^2 = 0.487$<br>$p < 0.001$ | F(1,29) = 25.064<br>$R^2 = 0.464$<br>$p < 0.001$ | F(1,29) = 42.516<br>$R^2 = 0.594$<br>$p < 0.001$ | F(1,29) = 25.357<br>$R^2 = 0.466$<br>$p < 0.001$ | F(1,29) = 27.676<br>$R^2 = 0.488$<br>$p < 0.001$ |
| C1q and CII | F(1,29) = 20.071<br>$R^2 = 0.409$<br>$p < 0.001$ | F(1,29) = 8.879<br>$R^2 = 0.234$<br>$p < 0.05$ | F(1,29) = 7.483<br>$R^2 = 0.205$<br>$p < 0.05$ | F(1,29) = 12.042<br>$R^2 = 0.293$<br>$p < 0.05$ | F(1,29) = 6.717<br>$R^2 = 0.188$<br>$p < 0.05$ | F(1,29) = 15.261<br>$R^2 = 0.345$<br>$p < 0.001$ |
| CD47 and age | F(1,29) = 13.825<br>$R^2 = 0.323$<br>$p < 0.001$ | F(1,29) = 23.227<br>$R^2 = 0.445$<br>$p < 0.001$ | F(1,29) = 26.519<br>$R^2 = 0.478$<br>$p < 0.001$ | F(1,29) = 18.775<br>$R^2 = 0.393$<br>$p < 0.001$ | F(1,29) = 21.040<br>$R^2 = 0.420$<br>$p < 0.001$ | F(1,29) = 21.080<br>$R^2 = 0.421$<br>$p < 0.001$ |
| CD47 and CII | F(1,29) = 0.897<br>$R^2 = 0.030$<br>$p = 0.351$ | F(1,29) = 2.963<br>$R^2 = 0.093$<br>$p = 0.096$ | F(1,29) = 12.032<br>$R^2 = 0.293$<br>$p < 0.05$ | F(1,29) = 7.216<br>$R^2 = 0.199$<br>$p < 0.05$ | F(1,29) = 6.685<br>$R^2 = 0.187$<br>$p < 0.05$]); | F(1,29) = 15.487<br>$R^2 = 0.348$<br>$p < 0.001$ |

we analyzed the colocalization of C1q with PSD95-positive puncta. As shown in Table 3, there was a significant increase in C1q-PSD95 colocalization in cortical layers 1–6 with age (Fig. 4a). Additionally, these increases were associated with cognitive impairment in all layers as shown in Table 3, (Fig. 4c).

**Table 3** Summary of statistics for % area of C1q-PSD95 colocalization and CD47-PSD95 colocalization associated with age and CII in cortical layers 1–6

| | Layer 1 | Layer 2 | Layer 3 | Layer 4 | Layer 5 | Layer 6 |
|---|---|---|---|---|---|---|
| C1q-PSD95 and age | $F(1,29)=20.509$<br>$R^2=0.414$<br>$p<0.001$ | $F(1,29)=10.079$<br>$R^2=0.397$<br>$p<0.001$ | $F(1,29)=22.709$<br>$R^2=0.439$<br>$p<0.001$ | $F(1,29)=38.898$<br>$R^2=0.573$<br>$p<0.001$ | $F(1,29)=18.948$<br>$R^2=0.395$<br>$p<0.001$ | [$F(1,29)=16.468$<br>$R^2=0.362$<br>$p<0.001$ |
| C1q-PSD95 and CII | $F(1,29)=16.847$<br>$R^2=0.367$<br>$p<0.001$ | $F(1,29)=6.099$<br>$R^2=0.174$<br>$p<0.05$ | $F(1,29)=6.540$<br>$R^2=0.184$<br>$p<0.05$ | $F(1,29)=10.108$<br>$R^2=0.258$<br>$p<0.05$ | $F(1,29)=4.820$<br>$R^2=0.143$<br>$p<0.05$ | $F(1,29)=6.725$<br>$R^2=0.188$<br>$p<0.05$ |
| CD47-PSD95 and age | $F(1,29)=3.776$<br>$R^2=0.115$<br>$p=0.062$ | $F(1,29)=4.216$<br>$R^2=0.127$<br>$p<0.05$ | $F(1,29)=3.667$<br>$R^2=0.112$<br>$p=0.065$ | $F(1,29)=4.564$<br>$R^2=0.136$<br>$p<0.05$ | $F(1,29)=8.929$<br>$R^2=0.235$<br>$p<0.05$ | $F(1,29)=8.716$<br>$R^2=0.231$<br>$p<0.05$ |
| CD47-PSD95 and CII | $F(1,29)=2.262$<br>$R^2=0.072$<br>$p=0.143$ | $F(1,29)=1.555$<br>$R^2=0.051$<br>$p=0.222$ | $F(1,29)=3.447$<br>$R^2=0.106$<br>$p<=0.074$ | $F(1,29)=3.271$<br>$R^2=0.101$<br>$p=0.081$ | $F(1,29)=4.124$<br>$R^2=0.124$<br>$p=0.052$ | $F(1,29)=4.813$<br>$R^2=0.142$<br>$p<0.05$ |

We then asked if the age-related decrease in CD47 is due to a concomitant impairment in synapse maintenance, by assessing colocalization of CD47 with PSD95. We found a significant decrease in CD47-PSD95 colocalization with age in layers 2 and 4–6 as shown in Table 3, (Fig. 4b). However, only significant correlation with cognitive impairment was found in layer 6 and approaching significance in layers 3, 4, and 5 as shown in Table 3, (Fig. 4d). There was no correlation with CSST total broken sets or % of perseverative errors out of total errors and C1q-PSD95% area or CD47-PSD95% area (data not shown).

## Microglia density, morphologies, and C1q expression in the dlPFC do not change with age

Since our results show the balance between C1q and CD47 favors phagocytosis conditions during aging, we investigated whether microglia morphology changed with age to reflect elevated phagocytic function. Here, we classified microglia according to Karperien morphology where homeostatic microglia with small somas and many, branching processes are ramified while phagocytic microglia are hypertrophic/amoeboid with enlarged somas and fewer, shorter processes [54], as shown in Fig. 5a. To further classify microglia, C1q+and C1q−expressing cells were counted. We found no significant differences in the density of ramified C1q−microglia [$F(1,30)=0.404$, $R^2=0.013$, $p=0.530$] (Fig. 5b), ramified C1q+[$F(1,30)=0.249$, $R^2=0.008$, $p=0.621$] (Fig. 5c), hypertrophic C1q−[$F(1,30)=0.343$, $R^2=0.011$, $p=0.563$] (Fig. 5d), or hypertrophic C1q+microglia [$F(1,30)=0.378$, $R^2=0.012$, $p=0.543$] (Fig. 5e) with age. Additionally, density of ramified or hypertrophic microglia and C1q presence did not correlate with CII score (ramified C1q−[$F(1,30)=0.029$, $R^2=0.001$, $p=0.866$], ramified C1q+[$F(1,30)=0.041$, $R^2=0.001$, $p=0.841$], hypertrophic C1q−[$F(1,30)=1.396$, $R^2=0.044$, $p=0.247$], hypertrophic C1q+[$F(1,30)=0.136$, $R^2=0.005$, $p=0.715$]), as shown in Fig. 5f–i. These results suggest that microglial phagocytic morphology does not increase with age or cognitive impairment in the dlPFC, and that microglia express stable C1q amounts with age.

## Stable microglial C1qA RNA but decreased neuronal CD47 RNA in the dlPFC with age

To examine the changes in microglial expression of C1q, RNAscope was used with a probe against *C1qA*, a subunit of the C1q molecule [48, 55]. This RNA expression was analyzed according to age and cognitive status by looking at animals grouped as young or old as well as cognitively spared or impaired. *C1qA* puncta were counted inside the soma of Iba1+cells, as shown in Fig. 6a and b. Consistent with our findings with IHC, results showed microglial expression of *C1qA* did not significantly change with age (16.9% increase in old animals, $p=0.683$; Fig. 6e) or with

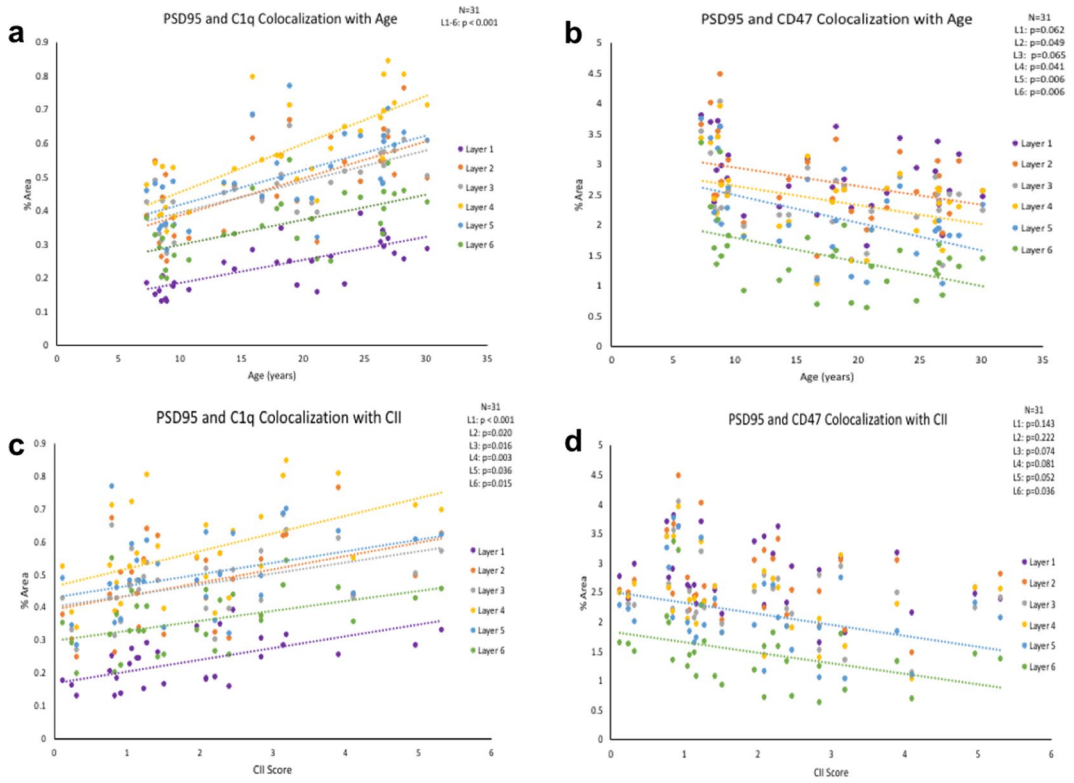


**Fig. 4** C1q-PSD95 and CD47-PSD95 colocalization with age and cognitive impairment. (**a**) % area of colocalized C1q and PSD95 signal increases significantly with age and (**c**) associates with cognitive impairment in cortical layers 1–6. (**b**) % area of colocalized CD47 and PSD95 signal significantly decreases with age in cortical layers 2, 4–6 and approaches significance in layers 1 and 3. (**d**) Decreased CD47 and PSD95 colocalization significantly correlates in layer 6 and approaches significance in layers 3–5

cognitive impairment (34.9% increase in impaired animals, $p=0.420$; Fig. 6f). To determine if neuronal expression of *CD47* was impaired with age, RNA was analyzed using a probe for *CD47* in MAP2+cells in the same tissue slices as the *C1qA* and Iba1 (Fig. 6a, b). Results showed significant decrease in expression of neuronal *CD47* mRNA (33.3% decrease, $p=0.001$) but this reduction in *CD47* expression was not associated with cognitive impairment (17.0% decrease, $p=0.231$), as shown in Fig. 6c and d, respectively. These data suggest that microglial C1q RNA expression remains stable in the dlPFC, but neurons have lower CD47 RNA expression with age.

## Discussion

### Summary of results

Age-related cognitive decline is associated with synapse loss in the monkey dlPFC [7, 20, 24, 49]. One possible mechanism for this synapse loss is that microglia, directed by immunologic proteins, aberrantly eliminate synapses. To assess this, "eat me" immunologic protein C1q and "don't eat me" protein CD47 and their localization to synapses were investigated in Area 46 of the dlPFC, an area critical for working memory and learning [7, 9]. C1q significantly increased in the dlPFC with age while CD47 decreased, and these changes correlated with age-related cognitive impairment. These results indicate that the aged dlPFC microenvironment favors phagocytosis of synaptic material. To determine if these molecules were targeting synapses, we analyzed the colocalization of C1q and CD47 with PSD95+synapses. Indeed, we found elevated C1q but reduced CD47 localization at PSD95+synapses with age. Importantly, PSD95+synapse loss was found within this C1q-enriched and CD47-deprived microenvironment, and increased C1q tagging of existing synapses was found with age. This synapse loss and C1q tagging were correlated with cognitive decline measured by a battery of

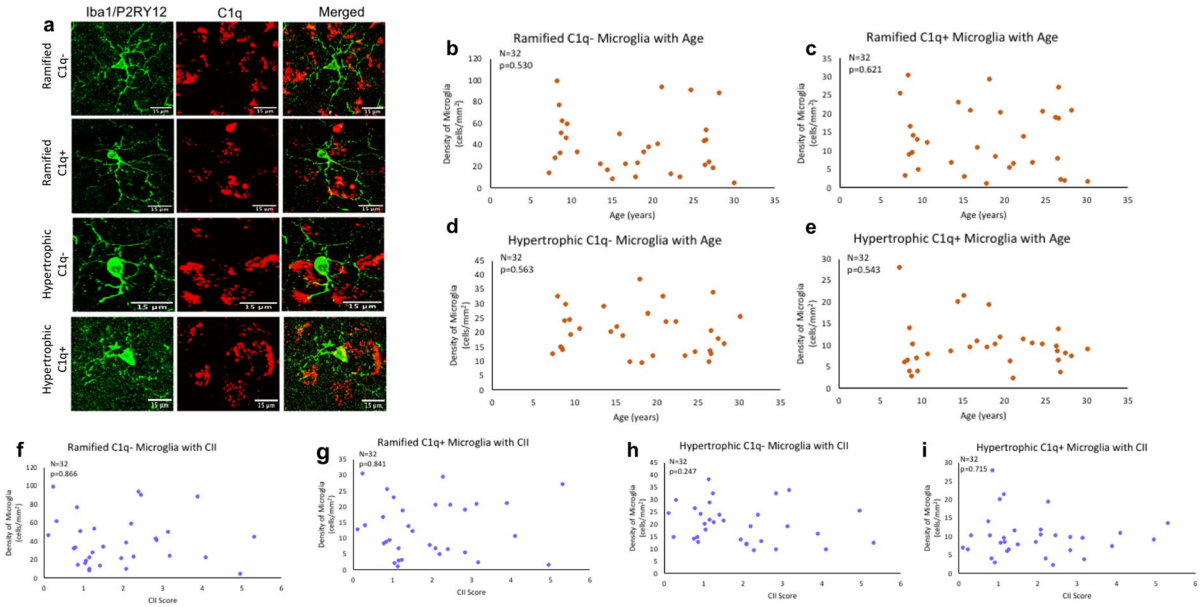


**Fig. 5** Classification and density of microglia morphology with age and related cognitive impairment. **a** Example images displaying ramified and hypertrophic morphology as well as C1q + or C1q − . **b**–**e** Ramified C1q −, ramified C1q +, hypertrophic C1q −, and hypertrophic C1q + microglia density did not change with age ($p > 0.05$). **f**–**i** Microglial morphology and C1q expression did not change with cognitive impairment ($p > 0.05$)

learning and memory tasks that yield a cognitive impairment index (CII).

To assess whether microglia are the culprits behind this synapse loss, we analyzed microglia morphology to determine if they are more phagocytically active with age. The density of Iba1 + microglia was counted and subdivided by morphology following the scheme of Karperien [54] who considered ramified microglia as homeostatic and hypertrophic microglia as phagocytic. Additionally, microglia were classified as C1q + or C1q − . Interestingly, we found no change in microglia morphology with age or expression of C1q. Finally, in terms of gene expression, we found reduced *CD47* RNA expression with age, but stable *C1qA* expression.

Overall, this suggests that neurons are less efficient at expressing *CD47* RNA with age, which leaves them more vulnerable to phagocytosis driven by C1q that increased with age and colocalized at PSD95 + synapses. Nevertheless, *C1q* was not upregulated in microglia, the main source of C1q [48].

## Aging and neuroinflammation

Age-related cognitive decline occurs in humans and monkeys that are free from neurodegenerative diseases, such as AD, and can be described as "normal" rather than neuropathological aging [14, 16]. In contrast to AD pathology, where neuron death results in major circuit disruption [56, 57], the "normal" aging brain has preserved neuronal numbers, but still exhibits structural disturbances such as spine loss, dendritic atrophy, and synapse loss in multiple areas including the dlPFC [20, 24, 49]. We found similar postsynaptic density loss with age across all six cortical layers of the dlPFC. Although the mechanism behind this loss is not known, evidence points to the involvement of the neuroimmune system in these structural alterations through microglia and microglia modulatory proteins as shown by the present study and elsewhere [28, 37, 38, 58, 59]. It is well established that microglia play a role in synapse formation and homeostasis, regulate neuronal activity, and modulate synaptic communication [60–62]. In particular, microglia roles in synaptic pruning have captured much attention [30–32] and neuron-microglia communication involves signaling from cytokines, chemokines, and complement components. During development, there is an upregulation in these modulatory proteins that direct synaptic pruning, but they return to normal levels after peak pruning periods

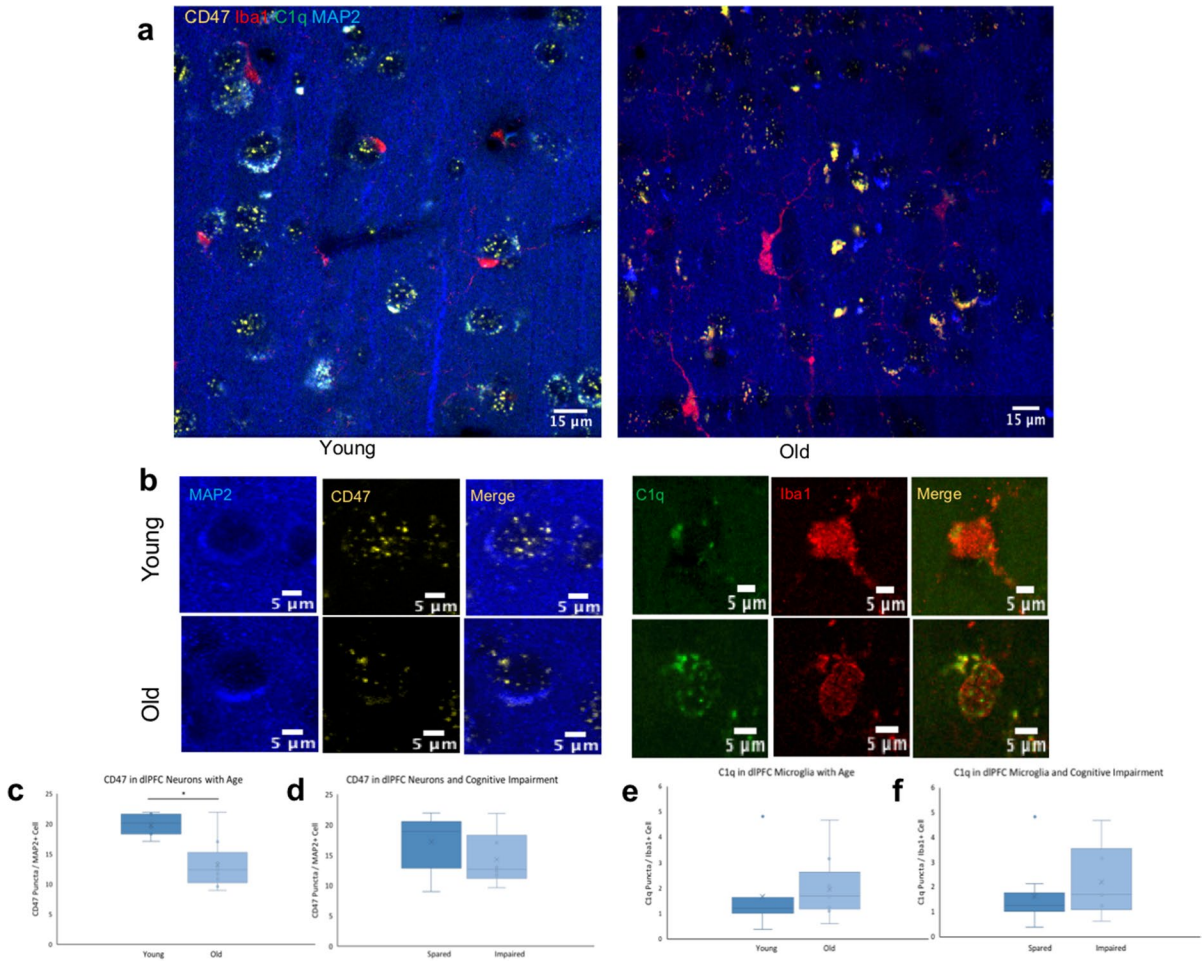


**Fig. 6** *C1qA* expression in microglia and *CD47* expression in neurons. **a**, **b** Staining of *C1qA* in Iba1 + microglia and *CD47* in MAP2 + neurons in young and old subjects. **c**, **d** Quantification of *CD47* in MAP2 + neurons with age and cognitive impairment, respectively. **e**, **f** *C1qA* puncta in Iba1 + microglia with age and cognitive impairment. Young < 10 years, old > 20 years; cognitively spared < 2.0, impaired > 2.0; $N = 16$, $^{*}p = 0.001$

[30, 35]. The reactivation of synapse elimination during aging may be a result of synapses becoming relatively inactive due to age-related myelin damage reducing synaptic drive [63, 64]. Alternatively, synapse removal may result from the same signaling components that are implicated in synapse pruning, which are upregulated by an age-related increase in neuroinflammation.

Similar to other organs in the body, the aging brain exhibits a phenomenon called inflammaging, where chronic, low level inflammation is present in the absence of injury or disease [65]. Neuroinflammation contributes to a number of neurodegenerative diseases and cognitive decline during aging [66, 67] and is characterized by microglial expression of pro-inflammatory markers such as IL-12, IL-1β, IL-23, and TNFα and complement components C1q and C3 in addition to reduced anti-inflammatory molecules such as IL-10 and IL-4 [68–71]. Moreover, upregulation of microglia genes of activation, phagocytosis, and lysosomal activity is found [28]. This chronic inflammation causes a negative feedback loop, where microglia are constantly both primed for phagocytosis and simultaneously upregulating and releasing inflammatory molecules into the microenvironment that could be damaging normal tissues [29, 72]. It has been hypothesized that elevation in pro-inflammatory molecules causes synaptic elimination conditions to

return, resulting in aberrant microglia-mediated synapse removal during aging [30, 38, 73].

Complement components including C1q and C3 are upregulated in aging mice and nonhuman primates. These components are understood to initiate synaptic pruning in the developing retina in an activity-dependent manner. However, this complement system is kept in check by opposing, inhibitory molecules that protect active synapses [35]. One inhibitory molecule, CD47, is a membrane-bound protein that is recognized by the signal regulatory protein receptor (SIRPα) on microglia, allowing for direct inhibition of phagocytosis [58, 74]. Here, we report C1q elevation in conjunction with reduced CD47 during aging in contrast to developmental synaptic pruning, where elevation of both occurs [30, 35]. Importantly, these proteins directly localized to synapses, where C1q localization was increased and CD47 localization was reduced. Furthermore, *CD47* RNA expression was significantly reduced in neurons. Together, these data suggest that neuronal efficiency in producing and expressing CD47 to protect itself is reduced with age. In the absence of CD47, C1q is able to increasingly opsonize to synapses and recruit the classical complement cascade to initiate phagocytosis. Thus, it appears that innate immune signaling is altered to favor synaptic elimination with aging. Importantly, the flip in C1q/CD47 balance with age correlates with cognitive impairment.

## Microglia elimination of synapses

Synaptic pruning is crucial during development to refine synaptic networks and regulate formation of appropriate, active connections [75, 76]. Without this process, aberrant connectivity may result in abnormal function and behavioral symptoms as seen in autism or schizophrenia [77, 78]. In the developing CNS, microglia are necessary for this process and beneficial in sculpting neural circuits. In disease states, increased complement components that modulate microglia are associated with synapse loss [30, 63, 73]. During aging, C1q localization to synapses is elevated, [37, 38] and it has been suggested that complement-mediated synapse elimination via microglia is associated with forgetfulness in adults [79]. This suggests the upregulation of complement components and localization to synapses could have harmful effects during aging and may underlie aberrant synapse loss via microglia during aging leading to cognitive impairment.

Microglia are key players in synapse elimination. Their processes are highly motile [80] and make frequent contact with synapses [81], which led to the hypothesis that microglia remove synapses. Indeed, pre- and postsynaptic material found within CD68 + microglial lysosomes [32, 79, 82] and within microglial processes [83] provide evidence that microglia engulf synaptic material. Furthermore, lack of microglial receptors CR3 and Cx3cr1 exhibits excessive immature synapses, indicating active microglial involvement of synaptic elimination [32, 83]. Increasing complement inhibitors results in decreased microglial engulfment of synapses [63]. Together, along with microglia's known role of phagocytosing unnecessary or harmful material from the microenvironment, these data indicate that microglia are the main cells engulfing synapses. However, the mechanisms underlying the process by which microglia ingest synapses leading to the presence of synaptic material within lysosomes and processes are unknown.

We hypothesized that, as with other material, microglia that phagocytosed synapses would become morphologically hypertrophic to envelope the synapse and eliminate it. Increased microglia expressions of activation markers such as LN-3 and MHC-II and phagocytic markers like galectin-3 are found in frontal white matter tracts [27, 72, 84, 85]. Additionally, increased hypertrophic microglia, characterized by enlarged soma and shortened processes, are found in both aging and neurodegenerative diseases [27, 59, 86–88]. Here, we sought to investigate if microglia morphology exhibited the same changes in aging dlPFC gray matter in response to increased phagocytic signaling. However, we found no changes in microglia morphology with age in the dlPFC gray matter. Further, we found no significant increase in C1q + microglia or upregulation of *C1qA* RNA expression. Thus, while there is increased C1q in the microenvironment and it localized to synapses, there is no change in microglial expression.

In contrast to axonal degeneration and myelin damage in the white matter [27, 64], it appears that synapse loss in gray matter of dlPFC is not associated with shifts in microglial morphologies from homeostatic to immune-activated phagocytic state. These data suggest that gray and white matter microglia are likely distinct phenotypes [89, 90], and that

downstream mechanisms and targets of C1q signaling can differ for myelin debris versus synapse elimination. Once C1q is released from microglia and tags debris, the downstream molecular targets of C1q can either promote anti-inflammatory (C3b) or exacerbate (C3a or C5) chronic pro-inflammatory signaling [91]. Thus, it will be important to determine if C1q signaling cascades and targets differ for microglial mediating synapse loss in the gray matter and myelin damage in the white matter with age. Indeed, our data point to an alternative hypothesis suggesting that microglia do not fully engulf synapses, but engage in partial phagocytosis, called trogocytosis [92]. Unlike phagocytosis, which involves engulfing cellular components greater than 1 μm, trogocytosis is the prompt "nibbling" of membrane components [93, 94]. Time-lapse light sheet microscopy of organotypic cultures revealed microglial trogocytosis of presynaptic structures but not postsynaptic [92]. In vivo, trogocytosis has also been observed at axonal presynaptic material in a complement-mediated manner [95]. If microglia are partially eliminating synaptic material, we would not have captured it here with only the assessment of hypertrophic morphology. These studies contradict previous research indicating that microglia contain both pre- and postsynaptic material inside their somas [32, 82]. More research is needed to clarify the mechanism by which microglia eliminate synaptic structures and which ones are preferentially targeted.

It is also important to note that microglia are not the sole mechanism for synapse elimination. Research suggests that astrocytes also eliminate synapses via the *Meg10* and *Mertk* pathways [96]. Additionally, astrocyte reactivity is induced by microglial secretion of inflammatory markers such as IL-1a, TNF, and C1q [97]. Thus, during aging, it is possible that astrocytes respond to the inflammatory environment and increased C1q levels by becoming reactive and eliminating synaptic elements. The dynamics between astrocyte and microglia in synapse removal is also unknown.

It is also of note that the current study focused on excitatory synapses marked by PSD95, but while inhibitory synapses are also decreased with age in monkey dlPFC [20], whether they are marked by C1q and eliminated by microglia is unknown. Finally, distinct cortical and subcortical pathways may be selectively vulnerable to age-related synapse loss, and therefore, may have distinct interactions with these neuroimmune signals. Previous studies have implicated weakening of cortico-cortical synapses of layer 3 dlPFC pyramidal neurons in age-related cognitive decline [98]. Additionally, studies have suggested that aging may be associated with particular vulnerability of thin spines [26, 49]. It is likely that the use of electron microscopy to assess how C1q/CD47 tagging relates to ultrastructural synaptic markers may help to decipher the effects of these neuroimmune signals on diverse types of synapses and cortical areas implicated in age-related cognitive decline and neurodegenerative diseases.

## Conclusions

In the present study, in normally aging rhesus monkeys in the absence of brain damage or neurodegenerative disease, we found age-related changes in the balance of complement components that regulate microglial phagocytosis. Interestingly, this change was associated with age-related synapse loss and cognitive decline. This investigation into both initiating complement component C1q and inhibiting signal CD47 during aging provides a novel observation that synapse loss is associated with both pro- and anti-elimination immunologic proteins, which may underlie a mechanism by which synapses are lost during aging even in the absence of neuron loss. Our findings also suggest that synapse maintenance requires proper balance of both pro-elimination signals and also inhibitory signals. Neuron-microglia communication is critical for maintaining cellular structures such as synaptic components [80]. Here, we demonstrate that dlPFC neurons are less capable of expressing protective CD47, while there is an increase in C1q in the environment. We hypothesize that reduction in neuronal CD47 expression may leave their membrane components, including synapses, more vulnerable to being tagged by C1q, thus being marked for elimination by microglia. While the present data did not show increased microglial phagocytic morphology, it is possible microglia employ trogocytosis to eliminate synapses by partial removal of synaptic material [92]. If this is the case, microglia morphology would not reveal the mechanism employed to eliminate synapses. Thus, markers of lysosomal and phagocytic activity should be investigated to determine if microglia are digesting synaptic material. Our findings provide the groundwork for further investigation into immunologic proteins and their interaction with neurons, microglia, and synapse loss. The present observations characterize only two molecules out of a large array of molecules regulating

synapses but do not show how these downstream complement proteins may contribute to age-related synapse loss and cognitive decline. It also suggests that this system may constitute a target for interventions aimed at slowing down or even reversing synapse loss and age-related cognitive decline.

**Acknowledgements** We would like to thank our technical staff Karen Slater, Penny Schultz, and Ashley Fair for their invaluable assistance.

**Author contribution** SD: conceptualization, methodology, investigation, analysis, original draft preparation. BC: visualization, investigation. CD: methodology, investigation. TM: methodology, resources. MM: methodology, review, and editing. FM: methodology, data curation. DR: review and editing, funding, supervision.

**Funding** This research was supported by NIH/NIA grants 1RF1AG062831 and 2RF1AG043640.

**Declarations**

**Competing interests** The authors declare no competing interests.

## References

1. Park DC, Reuter-Lorenz P. The adaptive brain: aging and neurocognitive scaffolding. In: Annual review of psychology. Palo Alto: Annual Reviews; 2009. p. 173–96.
2. Harada CN, Love MCN, Triebel KL. Normal cognitive aging. Clinics in Geriatric Medicine. 2013;29(4):737.
3. Freeman SH, et al. Preservation of neuronal number despite age-related cortical brain atrophy in elderly subjects without Alzheimer disease. J Neuropathol Exp Neurol. 2008;67(12):1205–12.
4. Morrison JH, Hof PR. Life and death of neurons in the aging brain. Science. 1997;278(5337):412–9.
5. Pakkenberg B, Gundersen HJG. Neocortical neuron number in humans: effect of sex and age. Journal of Comparative Neurology. 1997;384(2):312–20.
6. Terry RD, Deteresa R, Hansen LA. Neocortical cell counts in normal human adult aging. Ann Neurol. 1987;21(6):530–9.
7. Morrison JH, Baxter MG. The ageing cortical synapse: hallmarks and implications for cognitive decline. Nat Rev Neurosci. 2012;13(4):240–50.
8. Levy R, Goldman-Rakic PS. Association of storage and processing functions in the dorsolateral prefrontal cortex of the nonhuman primate. J Neurosci. 1999;19(12):5149–58.
9. Goldmanrakic PS. Topography of cognition - parallel distributed networks in primate association cortex. Annu Rev Neurosci. 1988;11:137–56.
10. Goldmanrakic PS. Cellular basis of working-memory. Neuron. 1995;14(3):477–85.
11. Rapp PR, Amaral DG. Evidence for task-dependent memory dysfunction in the aged monkey. J Neurosci. 1989;9(10):3568–76.
12. Herndon JG, et al. Patterns of cognitive decline in aged rhesus monkeys. Behav Brain Res. 1997;87(1):25–34.
13. Voytko ML. Impairments in acquisition and reversals of two-choice discriminations by aged rhesus monkeys. Neurobiol Aging. 1999;20(6):617–27.
14. Moss MB, Moore TL, Schettler SP, Killiany R, Rosene DL. Successful vs. unsuccessful aging in the rhesus monkey. In: Riddle DR, editor. Brain aging: Models, methods, and mechanisms. Boca Raton: CRC Press/Routledge/Taylor & Francis Group; 2007. p 21–38, Chapter 2. https://doi.org/10.1201/9781420005523.
15. Arnsten AFT, Goldmanrakic PS. Analysis of alpha-2 adrenergic agonist effects on the delayed nonmatch-to-sample performance of aged rhesus-monkeys. Neurobiol Aging. 1990;11(6):583–90.
16. Peters A, et al. Neurobiological bases of age-related cognitive decline in the rhesus monkey. J Neuropathol Exp Neurol. 1996;55(8):861–74.
17. Chiou KL, et al. Rhesus macaques as a tractable physiological model of human ageing. Philosophical Transactions of the Royal Society B-Biological Sciences. 1811;2020(375):9.
18. Peters A, et al. Are neurons lost from the primate cerebral cortex during normal aging? Cereb Cortex. 1998;8(4):295–300.
19. Giannaris EL, Rosene DL. A stereological study of the numbers of neurons and glia in the primary visual cortex across the lifespan of male and female rhesus monkeys. Journal of Comparative Neurology. 2012;520(15):3492–508.
20. Peters A, Sethares C, Luebke JI. Synapses are lost during aging in the primate prefrontal cortex. Neuroscience. 2008;152(4):970–81.
21. Medalla M, Luebke JI. Diversity of glutamatergic synaptic strength in lateral prefrontal versus primary visual cortices in the rhesus monkey. J Neurosci. 2015;35(1):112–27.
22. Chang W, et al. Age-related alterations to working memory and to pyramidal neurons in the prefrontal cortex of rhesus monkeys begin in early middle-age and are partially ameliorated by dietary curcumin. Neurobiol Aging. 2022;109:113–24.
23. Peters A, Sethares C. Aging and the myelinated fibers in prefrontal cortex and corpus callosum of the monkey. Journal of Comparative Neurology. 2002;442(3):277–91.
24. Hsu A, Luebke JI, Medalla M. Comparative ultrastructural features of excitatory synapses in the visual and frontal cortices of the adult mouse and monkey. Journal of Comparative Neurology. 2017;525(9):2175–91.
25. Moore TL, Medalla M, Ibanez S, Wimmer K, Mojica CA, Killiany RJ, Moss MB, Luebke JI, Rosene DL. Neuronal properties of pyramidal cells in lateral prefrontal cortex of the aging rhesus monkey brain are associated with performance deficits on spatial working memory but not executive function. Geroscience. 2023;45(3):1317–42. https://doi.org/10.1007/s11357-023-00798-2.
26. Young ME, et al. Differential effects of aging on dendritic spines in visual cortex and prefrontal cortex of the rhesus monkey. Neuroscience. 2014;274:33–43.

27. Shobin E, et al. Microglia activation and phagocytosis: relationship with aging and cognitive impairment in the rhesus monkey. Geroscience. 2017;39(2):199–220.
28. Safaiyan S, et al. Article white matter aging drives microglial diversity. Neuron. 2021;109(7):29.
29. Abraham J, et al. Aging sensitizes mice to behavioral deficits induced by central HIV-1 gp120. Neurobiol Aging. 2008;29(4):614–21.
30. Stevens B, et al. The classical complement cascade mediates CNS synapse elimination. Cell. 2007;131(6):1164–78.
31. Faust TE, Gunner G, Schafer DP. Mechanisms governing activity-dependent synaptic pruning in the developing mammalian CNS. Nat Rev Neurosci. 2021;22(11):657–73.
32. Schafer DP, et al. Microglia sculpt postnatal neural circuits in an activity and complement-dependent manner. Neuron. 2012;74(4):691–705.
33. Brown GC, Neher JJ. Microglial phagocytosis of live neurons. Nat Rev Neurosci. 2014;15(4):209–16.
34. Kanmogne M, Klein RS. Neuroprotective versus neuroinflammatory roles of complement: from development to disease. Trends Neurosci. 2021;44(2):97–109.
35. Lehrman EK, et al. CD47 protects synapses from excess microglia-mediated pruning during development. Neuron. 2018;100(1):120.
36. Oldenborg PA, Gresham HD, Lindberg FP. CD47-signal regulatory protein alpha (SIRP alpha) regulates Fc gamma and complement receptor-mediated phagocytosis. J Exp Med. 2001;193(7):855–61.
37. Datta D, et al. Classical complement cascade initiating C1q protein within neurons in the aged rhesus macaque dorsolateral prefrontal cortex. J Neuroinflammation. 2020;17(1):15.
38. Stephan AH, et al. A dramatic increase of C1q protein in the CNS during normal aging. J Neurosci. 2013;33(33):13460–74.
39. Moore TL, et al. Impairment in abstraction and set shifting in aged rhesus monkeys. Neurobiol Aging. 2003;24(1):125–34.
40. Moore TL, et al. A non-human primate test of abstraction and set shifting: an automated adaptation of the Wisconsin Card Sorting Test. J Neurosci Methods. 2005;146(2):165–73.
41. Killiany RJ, et al. Recognition memory function in early senescent rhesus monkeys. Psychobiology. 2000;28(1):45–56.
42. Moss MB, Rosene DL, Peters A. Effects of aging on visual recognition memory in the rhesus-monkey. Neurobiol Aging. 1988;9(5–6):495–502.
43. Moore TL, et al. Executive system dysfunction occurs as early as middle-age in the rhesus monkey. Neurobiol Aging. 2006;27(10):1484–93.
44. Estrada LI, et al. Evaluation of long-term cryostorage of brain tissue sections for quantitative histochemistry. J Histochem Cytochem. 2017;65(3):153–71.
45. Rosene DL, Roy NJ, Davis BJ. A cryoprotection method that facilitates cutting frozen-sections of whole monkey brains for histological and histochemical processing without freezing artifact. J Histochem Cytochem. 1986;34(10):1301–15.
46. Go V, et al. Extracellular vesicles from mesenchymal stem cells reduce microglial-mediated neuroinflammation after cortical injury in aged Rhesus monkeys. Geroscience. 2020;42(1):1–17.
47. Haynes SE, et al. The P2Y(12) receptor regulates microglial activation by extracellular nucleotides. Nat Neurosci. 2006;9(12):1512–9.
48. Fonseca MI, et al. Cell-specific deletion of C1qa identifies microglia as the dominant source of C1q in mouse brain. J Neuroinflammation. 2017;14:15.
49. Dumitriu D, et al. Selective changes in thin spine density and morphology in monkey prefrontal cortex correlate with aging-related cognitive impairment. J Neurosci. 2010;30(22):7507–15.
50. Kim EJ, Sheng M. PDZ domain proteins of synapses. Nat Rev Neurosci. 2004;5(10):771–81.
51. Bie BH, et al. Activation of mGluR1 mediates C1q-dependent microglial phagocytosis of glutamatergic synapses in Alzheimer's rodent models. Mol Neurobiol. 2019;56(8):5568–85.
52. Lee JH, et al. Complement C1q stimulates the progression of hepatocellular tumor through the activation of discoidin domain receptor 1. Sci Rep. 2018;8:11.
53. Zhang, L., Zhang, B., Dou, Z., Wu, J., Iranmanesh, Y., Jiang, B., Sun, C., Zhang, J. Immune checkpoint-associated locations of diffuse gliomas comparing pediatric with adult patients based on voxel-wise analysis. Front Immunol. 2021;12, 582594. https://doi.org/10.3389/fimmu.2021.582594.
54. Karperien A, Ahammer H, Jelinek HF. Quantitating the subtleties of microglial morphology with fractal analysis. Front Cell Neurosci. 2013;7:18.
55. Reid KBM, Porter RR. Subunit composition and structure of subcomponent CLQ of 1st component of human complement. Biochemical Journal. 1976;155(1):19–000.
56. Kitamura Y, Taniguchi T, Shimohama S. Apoptotic cell death in neurons and glial cells: implications for Alzheimer's disease. Jpn J Pharmacol. 1999;79(1):1–5.
57. Kril JJ, et al. Neuron loss from the hippocampus of Alzheimer's disease exceeds extracellular neurofibrillary tangle formation. Acta Neuropathol. 2002;103(4):370–6.
58. Gheibihayat SM, et al. CD47 in the brain and neurodegeneration: an update on the role in neuroinflammatory pathways. Molecules. 2021;26(13):15.
59. Shahidehpour RK, et al. Dystrophic microglia are associated with neurodegenerative disease and not healthy aging in the human brain. Neurobiol Aging. 2021;99:19–27.
60. Badimon A, et al. Negative feedback control of neuronal activity by microglia. Nature. 2020;586(7829):417.
61. Du YX, et al. Microglia maintain the normal structure and function of the hippocampal astrocyte network. Glia. 2022;70(7):1359–79.
62. Mordelt A, de Witte LD. Microglia-mediated synaptic pruning as a key deficit in neurodevelopmental disorders: hype or hope? Curr Opin Neurobiol. 2023;79:9.
63. Werneburg S, et al. Targeted complement inhibition at synapses prevents microglial synaptic engulfment and synapse loss in demyelinating disease. Immunity. 2020;52(1):167.
64. Bowley MP, et al. Age changes in myelinated nerve fibers of the cingulate bundle and corpus callosum in the rhesus monkey. Journal of Comparative Neurology. 2010;518(15):3046–64.
65. Franceschi C, et al. Inflammaging and anti-inflammaging: a systemic perspective on aging and longevity emerged from studies in humans. Mech Ageing Dev. 2007;128(1):92–105.

66. Ownby RL. Neuroinflammation and cognitive aging. Curr Psychiatry Rep. 2010;12(1):39–45.
67. Giunta B, Fernandez F, Nikolic WV, Obregon D, Rrapo E, Town T, Tan J. Inflammaging as a prodrome to Alzheimer's disease. J Neuroinflammation. 2008;5(51). https://doi.org/10.1186/1742-2094-5-51.
68. Norden DM, Godbout JP. Review: Microglia of the aged brain: primed to be activated and resistant to regulation. Neuropathol Appl Neurobiol. 2013;39(1):19–34.
69. Li QY, Barres BA. Microglia and macrophages in brain homeostasis and disease. Nat Rev Immunol. 2018;18(4):225–42.
70. Henry CJ, et al. Peripheral lipopolysaccharide (LPS) challenge promotes microglial hyperactivity in aged mice that is associated with exaggerated induction of both pro-inflammatory IL-1 beta and anti-inflammatory IL-10 cytokines. Brain Behav Immun. 2009;23(3):309–17.
71. Di Benedetto S, et al. Contribution of neuroinflammation and immunity to brain aging and the mitigating effects of physical and cognitive interventions. Neurosci Biobehav Rev. 2017;75:114–28.
72. Sloane JA, et al. Increased microglial activation and protein nitration in white matter of the aging monkey. Neurobiol Aging. 1999;20(4):395–405.
73. Stephan AH, Barres BA, Stevens B. The complement system: an unexpected role in synaptic pruning during development and disease. In: Hyman SE, editor. Annual review of neuroscience, vol. 35. Palo Alto: Annual Reviews; 2012. p. 369–89.
74. Zhang HY, et al. SIRP/CD47 signaling in neurological disorders. Brain Res. 2015;1623:74–80.
75. Katz LC, Shatz CJ. Synaptic activity and the construction of cortical circuits. Science. 1996;274(5290):1133–8.
76. Hua JYY, Smith SJ. Neural activity and the dynamics of central nervous system development. Nat Neurosci. 2004;7(4):327–32.
77. Obi-Nagata K, Temma Y, Hayashi-Takagi A. Synaptic functions and their disruption in schizophrenia: from clinical evidence to synaptic optogenetics in an animal model. Proceedings of the Japan Academy Series B-Physical and Biological Sciences. 2019;95(5):179–97.
78. Sacai H, et al. Autism spectrum disorder-like behavior caused by reduced excitatory synaptic transmission in pyramidal neurons of mouse prefrontal cortex. Nat Commun. 2020;11(1):15.
79. Wang C, et al. Microglia mediate forgetting via complement-dependent synaptic elimination. Science. 2020;367(6478):688.
80. Nimmerjahn A, Kirchhoff F, Helmchen F. Resting microglial cells are highly dynamic surveillants of brain parenchyma in vivo. Science. 2005;308(5726):1314–8.
81. Wake H, et al. Resting microglia directly monitor the functional state of synapses in vivo and determine the fate of ischemic terminals. J Neurosci. 2009;29(13):3974–80.
82. Schafer DP, et al. An engulfment assay: a protocol to assess interactions between CNS phagocytes and neurons. Jove-Journal of Visualized Experiments. 2014;88:12.
83. Paolicelli RC, et al. Synaptic pruning by microglia is necessary for normal brain development. Science. 2011;333(6048):1456–8.
84. Gefen T, et al. Activated microglia in cortical white matter across cognitive aging trajectories. Frontiers in Aging Neuroscience. 2019;11:8.
85. Sheffield LG, Berman NEJ. Microglial expression of MHC class II increases in normal aging of nonhuman primates. Neurobiol Aging. 1998;19(1):47–55.
86. Robillard KN, et al. Glial cell morphological and density changes through the lifespan of rhesus macaques. Brain Behav Immun. 2016;55:60–9.
87. Damani MR, et al. Age-related alterations in the dynamic behavior of microglia. Aging Cell. 2011;10(2):263–76.
88. Stojiljkovic MR, et al. Phenotypic and functional differences between senescent and aged murine microglia. Neurobiol Aging. 2019;74:56–69.
89. Lee J, et al. Heterogeneity of microglia and their differential roles in white matter pathology. CNS Neurosci Ther. 2019;25(12):1290–8.
90. Hart AD, et al. Age related changes in microglial phenotype vary between CNS regions: grey versus white matter differences. Brain Behav Immun. 2012;26(5):754–65.
91. Bohlson SS, et al. Complement, C1q, and C1 q-related molecules regulate macrophage polarization. Front Immunol. 2014;5:7.
92. Weinhard L, di Bartolomei G, Bolasco G, Machado P, Schieber NL, Neniskyte U, Exiga M, Vadisiute A, Raggioli A, Schertel A, Schwab Y, Gross C. Microglia remodel synapses by presynaptic trogocytosis and spine head filopodia induction. Nat Commun. 2018;9:1228. https://doi.org/10.1038/s41467-018-03566-5.
93. Dopfer EP, Minguet S, Schamel WWA. A new vampire saga: the molecular mechanism of T cell trogocytosis. Immunity. 2011;35(2):151–3.
94. Pham T, Mero P, Booth JW. Dynamics of macrophage trogocytosis of rituximab-coated B cells. PloS One. 2011;6(1):e14498. https://doi.org/10.1371/journal.pone.0014498.
95. Lim TKY, Ruthazer ES. Microglial trogocytosis and the complement system regulate axonal pruning in vivo. Elife. 2021;10:35.
96. Chung WS, et al. Astrocytes mediate synapse elimination through MEGF10 and MERTK pathways. Nature. 2013;504(7480):394.
97. Liddelow SA, et al. Neurotoxic reactive astrocytes are induced by activated microglia. Nature. 2017;541(7638):481–7.
98. Ibanez S, et al. Network models predict that pyramidal neuron hyperexcitability and synapse loss in the dlPFC lead to age-related spatial working memory impairment in rhesus monkeys. Front Comput Neurosci. 2020;13:21.